NIH Public Access
Author Manuscript
J Alzheimers Dis. Author manuscript; available in PMC 2013 January 03.

Published in final edited form as:
J Alzheimers Dis. 2012 ; 32(2): 467–478. doi:10.3233/JAD-2012-120424.

The Default Mode Network and Related Right Hemisphere Structures may be the Key Substrates of Dementia

Donald R. Royall[a,b,c,d,*], **Raymond F. Palmer**[c], **Eric D. Vidoni**[e], **Robyn A. Honea**[e], and **Jeffrey M. Burns**[e]

[a]Department of Psychiatry, The University of Texas Health Science Center, San Antonio, TX, USA

[b]Department of Medicine, The University of Texas Health Science Center, San Antonio, TX, USA

[c]Department of Family and Community Medicine, The University of Texas Health Science Center, San Antonio, TX, USA

[d]GRECC, the South Texas Veterans' Health System Audie L. Murphy Division, San Antonio, TX, USA

[e]Department of Neurology, KU Alzheimer and Memory Program, University of Kansas Medical Center, Kansas City, KS, USA

Abstract

We have employed structural equation models to explicitly distinguish dementia-relevant variance in cognitive task performance (i.e., d) from the variance that is unrelated to a dementing process (i.e., g′). Together g′ and d comprise Spearman's "g". Although d represents only a minor fraction of the total variance in cognitive task performance, it is more strongly associated with dementia severity than is g′. In this analysis, we replicate d in a new dataspace, the University of Kansas Brain Aging Project, and associate it specifically with regional grey matter atrophy by voxel-based morphometry of magnetic resonance imaging data. The latent variable d localizes to elements of the default mode network and related structures in the R hemisphere.

Keywords

Aging; cognition; dementia; g; functional status

INTRODUCTION

We have recently argued that dementing processes can be resolved to the cognitive correlates of functional status [1, 2]. To explore this hypothesis, we employed structural equation modeling (SEM) to explicitly distinguish dementia-relevant variance in cognitive task performance (i.e., d) from that which is unrelated to a dementing process (i.e., g′). The latent variables d and g′ are factors indicated by a battery's entire set of cognitive performance measures. However, only d is allowed to also be indicated by one or more functional status measures. Thus, d and not g′ represents "the cognitive correlates of

© 2012 – IOS Press and the authors. All rights reserved

*Correspondence to: Donald R. Royall, MD, The University of Texas Health Science Center, San Antonio, TX, USA. Tel.: +1 210 567 1255; Fax: +1 210 567 1269; royall@uthscsa.edu.

Authors' disclosures available online (http://www.jalz.com/disclosures/view.php?id=1418).

$watermark-text
$watermark-text
$watermark-text

$watermark-text

$watermark-text

$watermark-text

functional status", and is arguably essential to dementia case-finding [1]. Together, g′ and d effectively comprise Spearman's "g" (i.e., general intelligence) [3].

An important feature of Spearman's work was his demonstration of the "indifference of the indicator" to g. The content of cognitive measures is unimportant for the purposes of identifying g, because g affects performance on all tests. Jensen [4] has recently shown that the g factor extracted from one test battery will always be the same as that extracted from another, provided that the batteries are sufficiently diverse. Because d is a subset of g's variance, it may retain this property, which would facilitate its construction across datasets with differing cognitive and functional test batteries.

We recently validated d in the Texas Alzheimer's Research and Care Consortium (TARCC), a well characterized cohort of Alzheimer's disease (AD) cases and controls [2]. The latent variable d correlated significantly ($r = 0.84$, $p < 0.001$) with dementia severity, as assessed by the Clinical Rating Scale sum of boxes (CDR-SB) [5]. The latent variable g′ correlated weakly ($r = -0.18$, $p < 0.001$), despite the fact that it accounted for the majority of variance in cognitive test performance.

The structural brain correlates of d are unknown, but we suspect it to be related to the default mode network (DMN). The DMN is a network of highly interconnected brain regions that are active during wakeful introspection, and inactive during task specific processing. Its hubs include parts of the medial temporal lobe, the medial prefrontal cortex, the posterior cingulate, the precuneus, and the medial, lateral, and inferior parietal cortex [6].

Before the DMN's clinical salience was widely appreciated, we had specifically associated its key hubs with clinical dementia status, as rated by the CDR [7]. Since d is also very strongly associated with CDR scores, we hypothesize that its variance will map specifically to the DMN. In that case, it may be feasible to associate dementia status with the pathologies of a specific network and distinguish the dementing subset of neurodegenerative lesions from non-dementing disease burden affecting other structures.

In every dataspace we have examined, non-verbal cognitive measures load most strongly on d [2, 8]. In contrast, verbal measures load most strongly on g′. Non-verbal measures have been differentially associated with "fluid" intelligence, which declines with age, and age-related declines in functional status [9, 10], consistent with the so-called "right hemisphere theory of aging" [11]. Therefore, we also expect that d will be most strongly associated with DMN-related structures in the right (R) hemisphere.

METHODS

Sample

Participants were enrolled in the University of Kansas Brain Aging Project. Data used in these analyses were from selected individuals with early-stage AD (CDR 0.5 or 1.0, $n = 70$) or those without dementia (CDR 0.0, $n = 76$) aged 60 years and older. Study exclusions have been reported previously [12] and briefly include baseline included neurologic disease other than AD with the potential to impair cognition, current or past history of diabetes mellitus, recent history of cardiovascular disease, clinically significant depressive symptoms, and magnetic resonance imaging (MRI) exclusions among others. Portions of these data have been reported previously as part of a larger cohort [12–14]. Institutionally approved informed consent was obtained from all participants and their legal representative as appropriate before enrollment into the study.

$watermark-text

$watermark-text

$watermark-text

Clinical assessment

The clinical assessment included a semi-structured interview with the participant and a collateral source knowledgeable about the participant. Medications, past medical history, education, demographic information, and family history were collected from the collateral source. Dementia status of the participant was based on clinical evaluation [15]. Diagnostic criteria for AD require the gradual onset and progression of impairment in memory and at least one other cognitive and functional domain [16]. The CDR [17] assesses function in multiple domains and was used to assess dementia severity, such that CDR 0 indicates no dementia, CDR 0.5 indicates very mild, and CDR 1.0 indicates mild dementia. These methods have a diagnostic accuracy for AD of 93% and have been shown to be accurate in discriminating those with mild cognitive impairment (MCI) who have early stage AD [15, 18].

Cognitive assessment

A trained psychometrician administered a psychometric test battery that included common measures of memory: Wechsler Memory Scale–Revised Logical Memory IA (LMI) and IIA (LMII) [19]; the total free and cued Selective Reminding Task [20], language: Boston Naming Test–15 item (BNT15) [21], executive function: Trailmaking A and B [22], Category Fluency–Animals (CFAn) and Vegetables [23]; Stroop Color-Word Interference Test Color condition (StrCLR), word condition (StrWRD), and interference condition (StrINF) [24], and visuospatial ability: Weschler Adult Intelligence Scale-III Block Design [25].

Functional assessment

We used two common measures to index functional performance. First we administered the Alzheimer's Disease Cooperative Study Activities of Daily Living Scale for Mild Cognitive Impairment (ADCS-ADL) with information collected from the informant. The ADCS-ADL is a well characterized measure of independence in activities of daily living [26]. The 18-item measure is heavily weighted toward instrumental activities of daily living (IADL) such as meal preparation, travel outside the home, shopping, and performing household chores. Tasks are scored by increasing level of independence with greater scores reflecting more independence in IADL. Second, we administered the Nine-item modified Physical Performance Test (PPT) [12, 27]. Scores are given based on time to complete each task. The modified PPT is weighted toward basic (ADL) and includes writing a sentence, simulated eating, lifting a book and placing it on a shelf above shoulder height, putting on and removing a jacket, picking up a penny from the floor, turning 360°, ambulating 50 feet, five consecutive chair rises, and a progressive Romberg test.

Statistical approach

Latent variables of interest were constructed from confirmatory factor analyses performed in a SEM framework. All observed variables were adjusted for age, gender, and education. Residual covariances were empirically modeled to optimize fit. Model parameters were compared across models to ensure that model interpretation remained stable across alternative residual covariance structures. SEM was performed using AMOS software [28].

Missing data

Only the receiver-operating characteristic (ROC) analyses were limited to complete cases. Elsewhere, we used full information maximum likelihood (FIML) methods to address missing data. FIML uses the entire observed data matrix to estimate parameters with missing data. In contrast to listwise or pairwise deletion, FIML preserves the overall power, yields

$watermark-text

$watermark-text

$watermark-text

less biased parameter estimates, and is arguably superior to alternative methods, e.g., multiple imputation [29, 30].

Fit indices

The validity of SEM models was assessed using three common test statistics. A non-significant chi-square signifies that the data are consistent with the model [31]. The comparative fit index (CFI), with values ranging between zero and one, compares the specified model with a model of no change [32]. CFI values below 0.95 suggest model misspecification. Values of 0.95 or greater indicate adequate to excellent fit. A root mean square error of approximation (RMSEA) of 0.05 or less indicates a close fit to the data, with models below 0.05 considered "good" fit, and up to 0.08 as "acceptable" [33]. All three fit statistics should be simultaneously considered to assess the adequacy of the models to the data.

ROC curves

The diagnostic performance or accuracy of a test to discriminate diseased from normal cases can be evaluated using ROC curve analysis [34, 35]. Briefly the true positive rate (Sensitivity) is plotted as a function of the false positive rate (100-Specificity) for different cut-off points of a parameter. Each point on the ROC curve represents a sensitivity/specificity pairing corresponding to a particular decision threshold. The area under the ROC curve (AUC) is a measure of how well a parameter can distinguish between two diagnostic groups (diseased/normal). The analysis was performed in Statistical Package for the Social Sciences (SPSS) [36].

Neuroimaging

Baseline and follow-up whole brain structural MRI data were obtained using a Siemens 3.0 Tesla Allegra MRI Scanner. High-resolution T1 weighted anatomical images were acquired (magnetization-prepared rapid gradient echo [MPRAGE]; $1 \times 1 \times 1$ mm^3 voxels, repetition time [TR] = 2500, echo time [TE] = 4.38 ms, inversion time [TI] = 1,100 ms, field of view = 256×256, flip angle = 8°). Every scan was checked for image artifacts and gross anatomical abnormalities; three data sets were excluded for likely movement in the scanner. Data analysis was performed using the VBM5 toolbox (http://dbm.neuro.uni-jena.de), an extension of the SPM5 algorithms (Wellcome Department of Cognitive Neurology, London, UK) running under MATLAB 7.1 (The MathWorks, Natick, MA, USA).

Voxel-based morphometry (VBM) is a method for detecting differences in the volume of brain matter [37]. Our structural image processing method for VBM is detailed elsewhere [13].

Briefly, tissue classification, image registration, and MRI inhomogeneity bias correction were performed as part of the unified segmentation approach implemented in SPM5 [38]. We used the Hidden Markov Field model on the estimated tissue maps ($3 \times 3 \times 3$). Based on recommendations for aging and diseased populations, estimated tissue probability maps were written without making use of the International Consortium for Brain Mapping tissue priors to avoid a segmentation bias [39]. Images were then modulated and saved using affine registration plus non-linear spatial normalization [40]. The resulting gray matter volume maps were smoothed with a 10 mm FWHM Gaussian kernel before statistical analysis [41, 42].

Imaging statistics

We used a multiple regression model in SPM5 with g′, f, d factor scores and age and gender as covariates, centered on the mean. The absolute threshold masking was set at 0.10 to

$watermark-text

$watermark-text

$watermark-text

restrict each analysis to gray matter. Our primary interest was the positive relationship of d with regional brain volume, independent of the remaining regressors. Results were considered significant at $p < 0.05$, corrected for multiple comparisons (family-wise error), with clusters exceeding and extend of 50 voxles. Peak voxels are reported with reference to the MNI standard space and anatomic labels are reported with automated anatomical labeling [43] within the Pickatlas [44].

To confirm the specificity of d's association with the DMN, several masks were created using standard automated anatomic labeling [45] regions within the Wake Forest Pickatlas. Regions that best approximate the DMN as outlined by Buckner et al. [6] included bilateral medial superior frontal gyri, superior frontal orbital gyri, anterior cingulate, inferior parietal gyri, and middle temporal gyri (DMN). As controls, masks were created for primary motor cortex (bilateral precentral gyrus) (M1) and bilateral posterior cingulate/precuneus (PCP). Relative gray matter volume estimates within these three masks were corrected for age and gender.

The latent variable d's association with the DMN was tested by multiple regression in a SEM frame work. A latent variable representing "Global Atrophy" was created from the variance shared between d's structural eigenvariate, DMN, M1, and PCP. All observed variables were adjusted for age and gender.

RESULTS

First, we built a two factor model of 1) a latent variable "g", representing the variance shared across the cognitive measures in our battery (i.e., Spearman's "g"), and 2) a latent variable "f", representing the variance shared across all the individual items comprising the ADCS-ADL and PPT (i.e., the two functional status measures in our battery). Each cognitive measure loaded significantly on g (all $p < 0.001$). The latent variable g was most strongly loaded by LMII ($r = 0.88$), CFAn ($r = 0.75$), and BNT15 ($r = 0.75$) (i.e., "verbal" measures). Each functional status item loaded significantly on f (all $p < 0.05$), except ADCS-ADL 7: "Laundry", PPT5" "NAME", PPT6:"Circle Turn Score" and PPT8: "Sit to Stand Score". The latent variable f was most strongly loaded by ADCS-ADL9: "Telephone use" ($r = 0.84$), ADCS-ADL8: "Keeps Appointments" ($r = 0.75$), and ADCS-ADL11: "Talks about Current Events" ($r = 0.73$).

Next, we regressed g and f onto CDR-SB. Both were significantly and independently associated with CDR-SB (g: partial $r = -0.64$, $p < 0.001$; f: $r = -0.55$, $p < 0.001$). Together, they explained 71.7% of the variance in CDR-SB. However, fit was marginal (χ^2: 1226.34; df 653, $p \leq 0.001$; CMIN/DF = 1.88; RMSEA = 0.078; CFI = 0.803).

Next, we constructed a third factor, "d", representing the shared variance between cognitive performance and the functional status items (Fig. 1). In Fig. 1, rectangles represent observed variables, ovals represent latent constructs. Regression weights are represented by arrows. Standardized parameter estimates are presented. These can be interpreted as correlations of factor loadings, in the case of latent variable indicators.

The latent variable d uses functional status items as indicators rather than its correlates. This effectively parses the shared variance across the cognitive measures (i.e., g) into a larger fraction that is not related to functional status (i.e., g′), and a smaller fraction that is (i.e., d). This model's design (Fig. 1) suggests that d is orthogonal to g′ and f. We confirmed this by correlating d with each of the other two latent variables. No correlations were significant. This three factor model provides better fit to the data than the two factor model described above (χ^2: 686.53; df 591, $p \leq 0.001$; CMIN/DF = 1.16; RMSEA = 0.033; CFI = 0.967) (Table 3).

$watermark-text

$watermark-text

$watermark-text

All loadings on d were significant (all $p < 0.04$), except ADCS-ADL7: "Laundry". The latent variable d was most strongly loaded by StrWRD ($r = 0.808$; $p \leq 0.001$), StrCLR ($r = 0.797$; $p \leq 0.001$), and StrINT ($r = 0.787$; $p \leq 0.001$). The latent variable g′ was most strongly loaded by LM1 ($r = -0.644$; $p \leq 0.001$), and LMII ($r = -0.671$; $p \leq 0.001$). The latent variable f was again most strongly loaded by ADCS-ADL9: "Telephone use" ($r = -0.63$; $p \leq 0.001$), ADCS-ADL11: "Talks about Current Events" ($r = -0.57$; $p \leq 0.001$), and ADCS-ADL8: "Keeps Appointments" ($r = -0.54$; $p \leq 0.001$).

Next we examined the validity of our latent constructs in this dataspace. Consistent with our previous analysis in the TARCC dataset [2], d was strongly correlated with CDR-SB ($r = -0.80$) (Fig. 1; Table 4). Figure 2 presents ROC curves for the discrimination between AD cases and controls. Once again, d (i.e., the cognitive correlates of functional status) was best able to make this distinction (AUC = 0.995). The latent variable g′ (i.e., cognitive variance not related to functional status) and f (i.e., functional variance unrelated to cognition) were less accurate predictors of group membership. The latent variable d accurately distinguished AD from MCI (AUC = 0.89) and between MCI and controls (AUC = 0.91).

Figure 3 and Table 5 present the locations of peak correlation of gray matter volume with d. All associations are adjusted for g′, f, age, APOE $\varepsilon 4$ status, and gender. Visual inspection of Fig. 3 reveals a R hemisphere bias and overlap with elements of the DMN, notably the precuneus and anterior cingulate. This impression is supported by d's strong correlation with the DMN mask ($r = 0.57$; $R = 0.33$, $p < 0.001$) (Fig. 4). The latent variable d's specificity for DMN is indicated by the strong significant association between d′ and the relative volume extracted from the DMN mask. Outside of imaging space, this relationship is significant independent of M1, PCP, global atrophy, age, gender, and clinical diagnosis (partial $r = 0.63$, $p < 0.001$) (Fig. 5). This model has excellent fit ($\chi^2 = 0.129$, $p = 0.72$; CFI = 1.00; RMSEA = 0.00).

DISCUSSION

We recently proposed a re-conceptualization of "dementia" as the set of acquired disorders affecting the cognitive correlates of functional status (i.e., d). In this paper, we have associated this latent construct specifically with the DMN and related structures. We have also extended this work to a third dataspace, and provided additional support for d's validity as a "dementia"-specific construct.

The latent variable d appears robust. To date, we have successfully built it *ad hoc* in three datasets using whatever psychometric and functional status measures were at hand. In the present analysis, we were limited by the availability of only two functional status measures. As we previously reported in TARCC, f's factor loadings were attenuated by the introduction of d [2]. The latent variable d's strong associations with IADL and its strong association with non-verbal measures have been previously observed in other cohorts [2, 8] and may explain the apparent R hemisphere bias in its structural correlates.

This analysis provides additional support for d's validity as a proxy for "dementia". As in our earlier analysis [2], d is uniquely strongly associated with dementia status, as measured by CDR-SB. The latent variable d's AUC for the discrimination between AD and controls is very strong. The latent variable d appears to be singularly important to the distinction between AD cases and controls, while g′, representing the majority of variance in cognitive test performance, is not. This helps explain the relatively weak association between raw cognitive performance and functional outcomes [1].

As we expected, d mapped to elements of the DMN, notably the hippocampus, anterior cingulate, precuneus, middle temporal gyrus, and middle prefrontal cortex (Table 5) [6]. We

$watermark-text

$watermark-text

$watermark-text

were able to anticipate this finding *a priori* because of an earlier analysis of tauopathy's association with CDR scores [7]. In that analysis, we developed multivariate models to examine the association between CDR scale scores and the spatial distribution of paired helical filament tau pathology, obtained from 124 demented and non-demented elderly patients. Severity of tauopathy was examined in 14 cortical regions of interest (ROIs). Multiple-regression analyses were performed to determine the relative independent contributions of regional tauopathy to "dementia" (CDR ≥1.0).

Most structures made significant contributions to dementia. However, they were not independent. In multivariate models, only a single step (Step 7 in a hierarchical progression), which contained four ROIs, contributed significantly to dementia. A classification tree resulted in a single decision split, suggesting that only Step 7 ROIs need be considered when making this classification. A total of 89.4% of the cases were correctly classified ($p < 0.0001$). The key regions implicated by this analysis were the frontal cortex, the angular gyrus, the posterior cingulate, and the superior temporal cortex. We speculated that these (and the anterior cingulate, which was not included in that dataset) comprised a single cortical circuit related to the "executive control" of complex behavior.

In retrospect, these structures corresponded to hubs of the DMN. The latent variable d's strong association with that network supports the latter's critical role in determining a patient's dementia status. However, AD affects connectivity in several resting state networks, not only the DMN [46–48]. The anterior cingulate, orbito frontal cortex, and insula have been associated with the "salience" network [49]. Thus, d scores may be associated with a subset of structures contributing to more than one resting state network.

These networks are most properly defined by their connectivity rather than their constituent structures. It remains to be seen how d relates to connectivity measures. Grey matter atrophy and connectivity have different temporo-spatial trends [50]. Loss of connectivity in the DMN is associated voxelwise with amyloid-β deposition [51], and both are observed in cognitively normal persons [52]. Loss of connectivity also precedes atrophy in the anterior cingulate [53]. The latent variable d could be less sensitive to such preclinical AD changes as, by definition, they are occurring in the absence of IADL impairment, and many of d's constitutent indicators are vulnerable to floor effects.

The latent variable d's bias in favor of right hemisphere atrophy was also expected. Non-verbal measures tend to load strongly on d [2, 8]. Age-related cognitive changes resemble the effects of right hemisphere lesions, although compensatory L hemisphere activations may preserve cognitive performance in some cases [54]. However, all these models were age adjusted. The normal R hemisphere dominant hippocampal volume asymmetry is effaced as MCI progresses to AD [55, 56]. Positron emission tomography imaged amyloid-β deposition is largely symmetrical [57], but bilateral amyloid-β deposition in DMN-related structures is associated with greater right hemisphere atrophy [58]. This, and amyloid-β's co-localization with the DMN, suggests that amyloid-β may mediate d's association with atrophy in that network.

Non-demented APOE ε4 carriers have been reported to have reduced R hippocampal volumes, and abnormal R hippocampal activations by verbal memory tasks [59, 60]. However, in demented persons, APOE's effect on whole brain atrophy does not resemble d's [61], and left hippocampal atrophy is dominant [62]. Thus, the effects of APOE on AD diagnosis are probably not mediated through DMN atrophy and the d endophenotype, consistent with our APOE ε4 adjusted findings.

R hemisphere bias could also be introduced by d's association with IADL measures and functional status. Non-verbal measures generally explain more variance in IADL than do

$watermark-text

$watermark-text

$watermark-text

verbal [63, 64], and Chang et al. [65], using ADNI data, report associations between the variability in CDR functional status ratings and right hemisphere atrophy among cases with MCI. Thus, despite the fact that AD is associated with atrophy in both hemispheres, and relatively stable asymmetries across disease severity, the more disabling and thus "dementing" effects of those volume losses may still be mediated by the R hemisphere changes.

We also now report that d accurately distinguishes AD from MCI and between MCI and controls. Several studies have demonstrated changes by VBM across these clinical groups [66, 67]. However, a significant advantage of our latent variable approach to dementia case finding is that d's factor loadings can be used to calculate a continuously distributed "d score" endophenotype. ROC analysis could now be used establish d score thresholds that best distinguish the boundaries between normal performance, MCI, and dementia. Thus, it should be possible to precisely quantify the dementia status of any participant, rank order them for dementia severity, compare and or equate dementia severity across diagnoses or treatment groups, and evaluate clinical misclassification rates. This could allow the development of homogenous subject groups, for use in the clinical trials, and/or biomarker studies.

The disadvantage of this approach is that it requires an entire psychometric battery to construct d, despite the fact that relatively little of the battery's variance is related to it. However, Spearman's principal of "indifference of the indicator" suggests that future analyses may be able to reduce the battery, i.e., to a few widely used measures that load highly on d. This would minimize the assessment time needed to construct d and facilitate comparisons across samples.

In summary, we have explicitly distinguished dementia-relevant variance in cognitive task performance (i.e., d) from the variance that is unrelated to a dementing process (i.e., g′). We confirm in a new dataset that d is uniquely associated with dementia status and demonstrate its ability to distinguish MCI from both controls and AD cases. We find that d is specifically associated with the DMN and related structures in the R hemisphere. These results have implications for the clinical assessment of dementia. Our ability to distinguish d specifically could improve our ability to model dementing processes and establish their specific bio-markers.

Acknowledgments

This study was made possible by the Julia and Van Buren Parr endowment for the study of Alzheimer's disease. The sponsor had no role in study design, data collection and analysis, decision to publish, or preparation of the manuscript. The Brain Aging Project is supported by grants R03AG026374 and R21AG029615 from the National Institutes of Aging, grant K23NS058252 from the National Institute on Neurological Disorders and Stroke. The University of Kansas General Clinical Research Center (M01RR023940) provided essential space, expertise, and nursing support. Dr. Burns and Vidoni are supported by the University of Kansas Alzheimer's Disease Center (P30AG035982). Dr. Burns is also supported by R01AG034614 and R01AG033673. Dr. Vidoni is also supported by the Heartland Institute for Clinical & Translational Research, University of Kansas Medical Center's CTSA, KL2 TR000119 & UL1 TR00001. Dr. Honea is supported by K01AG035042.

References

1. Royall DR, Lauterbach EC, Kaufer DI, Malloy P, Coburn KL, Black KJ. The cognitive correlates of functional status: A review from the Committee on Research of the American Neuropsychiatric Association. J Neuropsychiatry Clin Neurosci. 2007; 19:249–265. [PubMed: 17827410]
2. Royall DR, Palmer RF, O'Bryant S. Validation of a latent variable representing the dementing process. J Alzheimers Dis. 2012; 30:639–649. [PubMed: 22451315]

$watermark-text
$watermark-text
$watermark-text

3. Spearman, C. The Abilities of Man: Their Nature and Measurement. Macmillan & Co; London: 1932.
4. Jensen AR. Understanding g in terms of information processing. Educ Psychology Rev. 1992; 4:271–308.
5. Hughes CP, Berg L, Danziger WL, Coben LA, Martin RL. A new clinical scale for the staging of dementia. Br J Psychiatry. 1982; 140:566–572. [PubMed: 7104545]
6. Buckner RL, Andrews-Hanna JR, Schacter DL. The brain's default network: Anatomy, function, and relevance to disease. Ann NY Acad Sci. 2008; 1124:1–38. [PubMed: 18400922]
7. Royall DR, Palmer R, Mulroy A, Polk MJ, Román GC, David J-P, Delacourte A. Pathological determinants of clinical dementia in Alzheimer's disease. Exp Aging Res. 2002; 28:143–162. [PubMed: 11928525]
8. Royall DR, Palmer RF. Getting past "g": Testing a new model of dementing processes in non-demented persons. J Neuropsychiatry Clin Neurosci. 2012; 24:37–46. [PubMed: 22450612]
9. Artero S, Touchon J, Ritchie K. Disability and mild cognitive impairment: A longitudinal population-based study. Int J Geriatr Psychiatr. 2001; 16:1092–1097.
10. Royall DR, Palmer R, Chiodo LK, Polk M. Normal rates of cognitive change in successful aging: The Freedom House Study. J Int Neuropsychol Soc. 2005; 11:899–909. [PubMed: 16519269]
11. Elias JW. Lifespan perspective on cerebral asymmetry and information processing with an emphasis on the aging adult. Century Syst Commun Elderly. 1979; 18:187–201.
12. Burns JM, Cronk BB, Anderson HS, Donnelly JE, Thomas GP, Harsha A, Brooks WM, Swerdlow RH. Cardiorespiratory fitness and brain atrophy in early Alzheimer disease. Neurol. 2008; 71:210–216.
13. Honea RA, Thomas GP, Harsha A, Anderson HS, Donnelly JE, Brooks WM, Burns JM. Cardiorespiratory fitness and preserved medial temporal lobe volume in Alzheimer disease. Alzheimer Dis Assoc Disord. 2009; 23:188–197. [PubMed: 19812458]
14. Vidoni ED, Honea RA, Billinger SA, Swerdlow RH, Burns JM. Cardiorespiratory fitness is associated with atrophy in Alzheimer's and aging over 2 years. Neurobiol Aging. 2012; 33:1624–1632. [PubMed: 21531480]
15. Morris JC, Storandt M, Miller JP, McKeel DW, Price JL, Rubin EH, Berg L. Mild cognitive impairment represents early-stage Alzheimer disease. Arch Neurol. 2001; 58:397–405. [PubMed: 11255443]
16. McKhann G, Drachman D, Folstein M, Katzman R, Price D, Stadlan EM. Clinical diagnosis of Alzheimer's disease: Report of the NINCDS-ADRDA Work Group under the auspices of Department of Health and Human Services Task Force on Alzheimer's disease. Neurology. 1984; 34:939–944. [PubMed: 6610841]
17. Morris JC. The Clinical Dementia Rating (CDR): Current version and scoring rules. Neurology. 1993; 43:2412–2414. [PubMed: 8232972]
18. Berg L, McKeel DW Jr, Miller JP, Storandt M, Rubin EH, Morris JC, Baty J, Coats M, Norton J, Goate AM, Price JL, Gearing M, Mirra SS, Saunders AM. Clinicopathologic studies in cognitively healthy aging and Alzheimer disease: Relation of histologic markers to dementia severity, age, sex, and apolipoprotein E genotype. Arch Neurol. 1998; 55:326–335. [PubMed: 9520006]
19. Wechsler, D.; Stone, CP. Manual: Wechsler Memory Scale. Psychological Corporation; New York: 1973.
20. Grober E, Buschke H, Crystal H, Bang S, Dresner R. Screening for dementia by memory testing. Neurol. 1988; 38:900–903.
21. Goodglass, H.; Kaplan, E. Boston Naming Test scoring booklet. Lea & Febiger; Philadelphia: 1983.
22. Hänninen T, Reinikainen KJ, Helkala EL, Koivisto K, Mykkänen L, Laakso M, Pyörälä K, Riekkinen PJ. Subjective memory complaints and personality traits in normal elderly subjects. J Am Geriatr Soc. 1994; 42:1–4. [PubMed: 8277103]
23. Armitage SG. An analysis of certain psychological tests used in the evaluation of brain injury. Psychol Monographs. 1946; 60:1–48.
24. Stroop J. Studies of interference in serial verbal reactions. J Exp Psychol. 1935; 18:643–662.

$watermark-text

$watermark-text

$watermark-text

25. Wechsler, D. Manual: Wechsler Adult Intelligence Scale. Psychological Corporation; New York: 1955.
26. Galasko D, Bennett D, Sano M, Ernesto C, Thomas R, Grundman M, Ferris S. An inventory to assess activities of daily living for clinical trials in Alzheimer's disease. The Alzheimer's Disease Cooperative Study. Alz Dis Assoc Disord. 1997; 11 (Suppl 2):S33–S39.
27. Reuben DB, Siu AL. An objective measure of physical function of elderly outpatients. The Physical Performance Test. J Am Geriatr Soc. 1990; 38:1105–1112. [PubMed: 2229864]
28. Arbuckle, JL. Analysis of Moment Structures-AMOS (Version 7.0) [Computer Program]. SPSS; Chicago: 2006.
29. Schafer JL, Graham JW. Missing data: Our view of the state of the art. Psychol Methods. 2002; 7:147–177. [PubMed: 12090408]
30. Graham JW. Missing data analysis: Making it work in the real world. Annu Rev Psychol. 2009; 6:549–576. [PubMed: 18652544]
31. Bollen, KA.; Long, JS. Testing Structural Equation Models. Sage Publications; Thousand Oaks, CA: 1993.
32. Bentler PM. Comparative fit indexes in structural models. Psychol Bull. 1990; 107:238–246. [PubMed: 2320703]
33. Browne, M.; Cudeck, R. Alternative ways of assessing model fit. In: Bollen, KA.; Long, JS., editors. Testing structural equation models. Sage Publications; Thousand Oaks, CA: 1993. p. 136-162.
34. Metz CE. Basic principles of ROC analysis. Sem Nuc Med. 1978; 8:283–298.
35. Zweig MH, Campbell G. Receiver-operating characteristic (ROC) plots: A fundamental evaluation tool in clinical medicine. Clin Chem. 1993; 39:561–577. [PubMed: 8472349]
36. PASW Statistics 18, Release Version 18.0.0. SPSS, Inc; Chicago, IL: 2009. http://www.spss.com
37. Honea R, Crow TJ, Passingham D, Mackay CE. Regional deficits in brain volume in schizophrenia: A meta-analysis of voxel-based morphometry studies. Am J Psychiatry. 2005; 162:2233–2245. [PubMed: 16330585]
38. Ashburner J, Friston KJ. Unified segmentation. Neuroimage. 2005; 26:839–851. [PubMed: 15955494]
39. Gaser C, Altaye M, Wilke M, Holland SK. Unified segmentation without tissue priors. Neuroimage. 2007; 36(Suppl 1):S68.
40. Wilke M, Holland SK, Altaye M, Gaser C. Template-O-Matic: A toolbox for creating customized pediatric templates. Neuroimage. 2008; 41:903–913. [PubMed: 18424084]
41. Buckholtz JW, Meyer-Lindenberg A, Honea RA, Straub RE, Pezawas L, Egan MF, Vakkalanka R, Kolachana B, Verchinski BA, Sust S, Mattay VS, Weinberger DR, Callicott JH. Allelic variation in RGS4 impacts functional and structural connectivity in the human brain. J Neurosci. 2007; 27:1584–1593. [PubMed: 17301167]
42. Boyke J, Driemeyer J, Gaser C, Büchel C, May A. Training-induced brain structure changes in the elderly. J Neurosci. 2008; 28:7031–7035. [PubMed: 18614670]
43. Lancaster JL, Rainey LH, Summerlin JL, Freitas CS, Fox PT, Evans AC, Toga AW, Mazziotta JC. Automated labeling of the human brain: A preliminary report on the development and evaluation of a forward-transform method. Hum Brain Mapp. 1997; 5:238–242. [PubMed: 20408222]
44. Maldjian JA, Laurienti PJ, Kraft RA, Burdette JH. An automated method for neuroanatomic and cytoarchitectonic atlas-based interrogation of fMRI data sets. Neuroimage. 2003; 19:1233–1239. [PubMed: 12880848]
45. Tzourio-Mazoyer N, Landeau B, Papathanassiou D, Crivello F, Etard O, Delcroix N, Mazoyer B, Joliot M. Automated anatomical labeling of activations in SPM using a macroscopic anatomical parcellation of the MNI MRI single-subject brain. Neuroimage. 2002; 15:273–289. [PubMed: 11771995]
46. Sperling RA, Dickerson BC, Pihlajamaki M, Vannini P, LaViolette PS, Vitolo OV, Hedden T, Becker JA, Rentz DM, Selkoe DJ, Johnson KA. Functional alterations in memory networks in early Alzheimer's disease. Neuromolecular Med. 2010; 12:27–43. [PubMed: 20069392]

$watermark-text

$watermark-text

$watermark-text

47. Agosta F, Pievani M, Geroldi C, Copetti M, Frisoni GB, Filippi M. Resting state fMRI in Alzheimer's disease: Beyond the default mode network. Neurobiol Aging. 2012; 33:1564–1578. [PubMed: 21813210]
48. Liang P, Wang Z, Yang Y, Li K. Three subsystems of the inferior parietal cortex are differently affected in mild cognitive impairment. J Alzheimers Dis. 2012; 30:475–487. [PubMed: 22451310]
49. Seeley WW, Menon V, Schatzberg AF, Keller J, Glover GH, Kenna H, Reiss AL, Greicius MD. Dissociable intrinsic connectivity networks for salience processing and executive control. J Neurosci. 2007; 27:2349–2356. [PubMed: 17329432]
50. Shin J, Kepe V, Small GW, Phelps ME, Barrio JR. Multimodal imaging of Alzheimer pathophysiology in the brain's default mode network. Int J Alzheimers Dis. 2011; 2011:687945. [PubMed: 21629709]
51. Buckner RL, Sepulcre J, Talukdar T, Krienen FM, Liu H, Hedden T, Andrews-Hanna JR, Sperling RA, Johnson KA. Cortical hubs revealed by intrinsic functional connectivity: Mapping, assessment of stability, and relation to Alzheimer's disease. J Neurosci. 2009; 29:1860–1873. [PubMed: 19211893]
52. Sheline YI, Raichle ME, Snyder AZ, Morris JC, Head D, Wang S, Mintun MA. Amyloid plaques disrupt resting state default mode network connectivity in cognitively normal elderly. Biol Psychiatry. 2010; 67:584–587. [PubMed: 19833321]
53. Bozzali M, Padovani A, Caltagirone C, Borroni B. Regional grey matter loss and brain disconnection across Alzheimer disease evolution. Curr Med Chem. 2011; 18:2452–2458. [PubMed: 21568913]
54. Dolcos F, Rice HJ, Cabeza R. Hemispheric asymmetry and aging: Right hemisphere decline or asymmetry reduction. Neurosci Biobehav Rev. 2002; 26:819–825. [PubMed: 12470693]
55. Shi F, Liu B, Zhou Y, Yu C, Jiang T. Hippocampal volume and asymmetry in mild cognitive impairment and Alzheimer's disease: Meta-analyses of MRI studies. Hippocampus. 2009; 19:1055–1064. [PubMed: 19309039]
56. Kim JH, Lee JW, Kim GH, Roh JH, Kim MJ, Seo SW, Kim ST, Jeon S, Lee JM, Heilman KM, Na DL. Cortical asymmetries in normal, mild cognitive impairment, and Alzheimer's disease. Neurobiol Aging. 2012; 33:1959–1966. [PubMed: 21907459]
57. Raji CA, Becker JT, Tsopelas ND, Price JC, Mathis CA, Saxton JA, Lopresti BJ, Hoge JA, Ziolko SK, DeKosky ST, Klunk WE. Characterizing regional correlation, laterality and symmetry of amyloid deposition in mild cognitive impairment and Alzheimer's disease with Pittsburgh Compound B. J Neurosci Methods. 2008; 172:277–282. [PubMed: 18582948]
58. Tosun D, Schuff N, Mathis CA, Jagust W, Weiner MW. Alzheimer's Disease NeuroImaging Initiative . Spatial patterns of brain amyloid-beta burden and atrophy rate associations in mild cognitive impairment. Brain. 2011; 134:1077–1088. [PubMed: 21429865]
59. Han SD, Houston WS, Jak AJ, Eyler LT, Nagel BJ, Fleisher AS, Brown GG, Corey-Bloom J, Salmon DP, Thal LJ, Bondi MW. Verbal paired-associate learning by APOE genotype in nondemented adults: fMRI evidence of a right hemispheric compensatory response. Neurobiol Aging. 2007; 28:238–247. [PubMed: 16434125]
60. Lind J, Larsson A, Persson J, Ingvar M, Nilsson LG, Bäckman L, Adolfsson R, Cruts M, Sleegers K, Van Broeckhoven C, Nyberg L. Reduced hippocampal volume in non-demented carriers of the apolipoprotein E epsilon4: Relation to chronological age and recognition memory. Neurosci Lett. 2006; 396:23–27. [PubMed: 16406347]
61. Pievani M, Rasser PE, Galluzzi S, Benussi L, Ghidoni R, Sabattoli F, Bonetti M, Binetti G, Thompson PM, Frisoni GB. Mapping the effect of APOE epsilon4 on gray matter loss in Alzheimer's disease *in vivo*. Neuroimage. 2009; 45:1090–1098. [PubMed: 19349226]
62. Pievani M, Galluzzi S, Thompson PM, Rasser PE, Bonetti M, Frisoni GB. APOE4 is associated with greater atrophy of the hippocampal formation in Alzheimer's disease. Neuroimage. 2011; 55:909–919. [PubMed: 21224004]
63. Royall DR, Palmer R, Chiodo LK, Polk M. Normal rates of cognitive change in successful aging: The Freedom House Study. J Int Neuropsychol Soc. 2005; 11:899–909. [PubMed: 16519269]
64. Artero S, Touchon J, Ritchie K. Disability and mild cognitive impairment: A longitudinal population-based study. Int J Geriatr Psychiatry. 2001; 16:1092–1097. [PubMed: 11746656]

65. Chang YL, Bondi MW, McEvoy LK, Fennema-Notestine C, Salmon DP, Galasko D, Hagler DJ Jr, Dale AM. Alzheimer's Disease Neuroimaging Initiative. Global clinical dementia rating of 0.5 in MCI masks variability related to level of function. Neurology. 2011; 76:652–659. [PubMed: 21321338]

66. Whitwell JL, Przybelski SA, Weigand SD, Knopman DS, Boeve BF, Petersen RC, Jack CR Jr. 3D maps from multiple MRI illustrate changing atrophy patterns as subjects progress from mild cognitive impairment to Alzheimer's disease. Brain. 2007; 130:1777–1786. [PubMed: 17533169]

67. Ferreira LK, Diniz BS, Forlenza OV, Busatto GF, Zanetti MV. Neurostructural predictors of Alzheimer's disease: A meta-analysis of VBM studies. Neurobiol Aging. 2011; 32:1733–1741. [PubMed: 20005012]

$watermark-text

$watermark-text

$watermark-text

$watermark-text
$watermark-text
$watermark-text

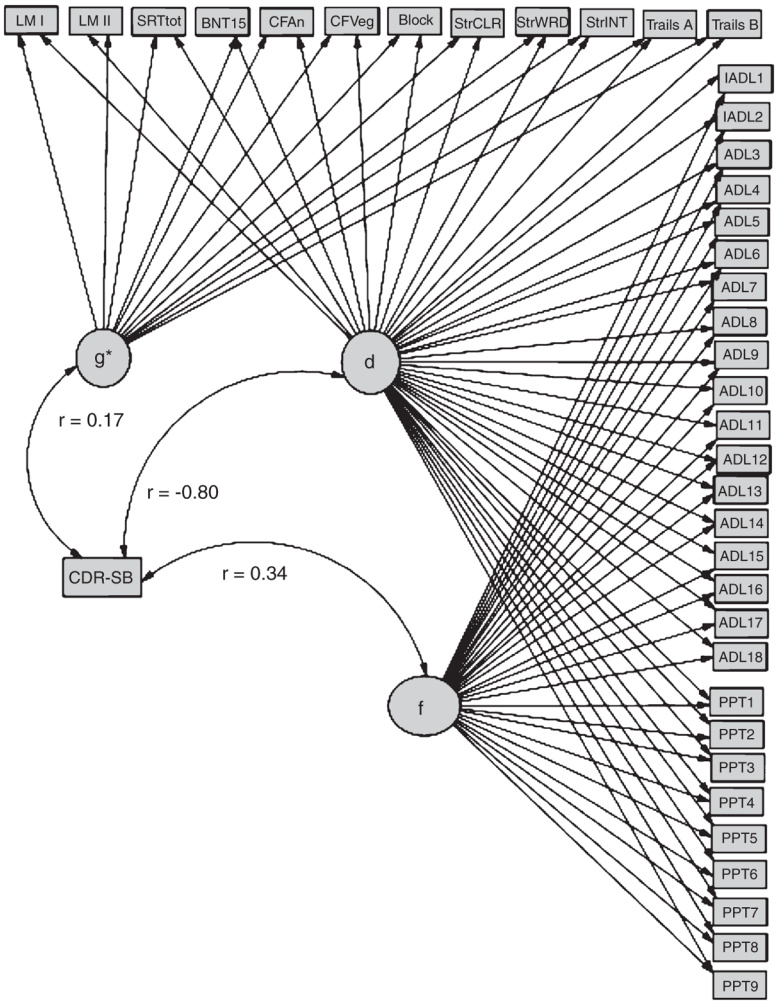

Fig. 1.

δ Correlates strongly with CDR-SB. ADL = Alzheimer's Disease Cooperative Study Activities of Daily Living Scale for Mild Cognitive Impairment; ADL1, Personal Belongings; ADL2, Clothes Selection; ADL3, Dressing; ADL4, Cleaning; ADL5, Balance Checkbook; ADL6, Writing; ADL7, Laundry; AD: 8, Keep Appointments; ADL9, Telephone Use; ADL10, Meal Preparation; ADL11, Travel Outside the Home; ADL12, Talk about Current Events; ADL13, Reading; ADL14, Watching TV; ADL15 = Shopping; ADL16, Left Alone; ADL17, Appliance Use; ADL 18, Hobbies; BLOCK, WAIS-R Block Design; BNT15, Boston Naming Test (15 item); CFAn, Category Fluency: Animals; CFVeg, Category Fluency: Vegetables; LMI, Wechsler Memory Scale–Revised Logical Memory; LMII, Wechsler Memory Scale–Revised Logical Memory Delayed; PPT, modified Physical Performance Test; PPT1, Writing a Sentence; PPT2, Bean Transfer; PPT3, Lifting a Book and Placing it on a Shelf above Shoulder Height; PPT4, Putting on and Removing a Jacket; PPT5, Picking up a Penny from the Floor; PPT6, Turning 360°; PPT7, Ambulating 50 feet; PPT8, Five Consecutive Chair Rises; PPT9, Progressive Romberg Test; SRTtot, Selective Reminding Task Free Recall Total; StrCLR, Stroop Color Task; StrINT, Stroop Color-Word Interference Task; StrWRD, Stroop Task; Trails A, Trail Making Test part A; Trails B, Trail Making Test part B.

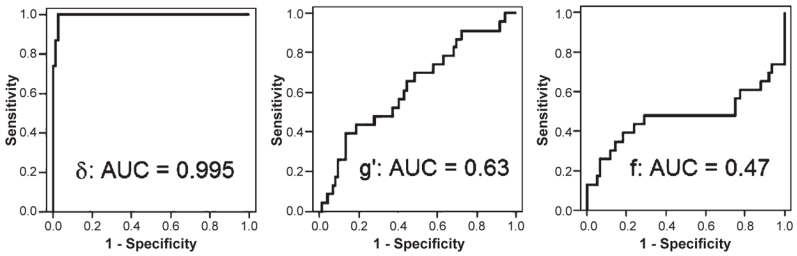

Fig. 2.
ROC curves for the discrimination between AD cases and controls*. *Each latent variable predictor is adjusted for the other two.

$watermark-text
$watermark-text
$watermark-text

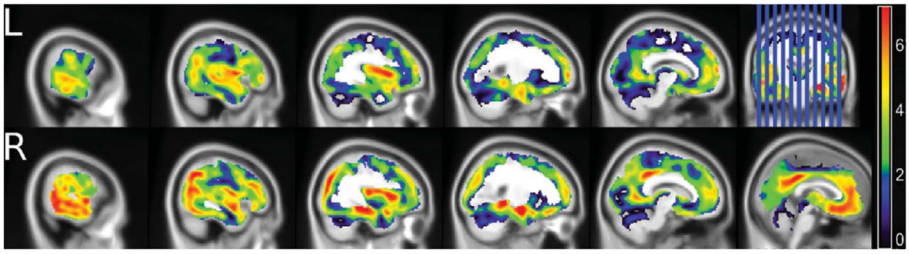

Fig. 3.

Regional cortical atrophy associated specifically with d*. *Adjusted for age, gender, APOE-ε4 carrier status, g' and f. Note R hemisphere predominance and overlap with elements of the Default Mode Network.

$watermark-text
$watermark-text
$watermark-text

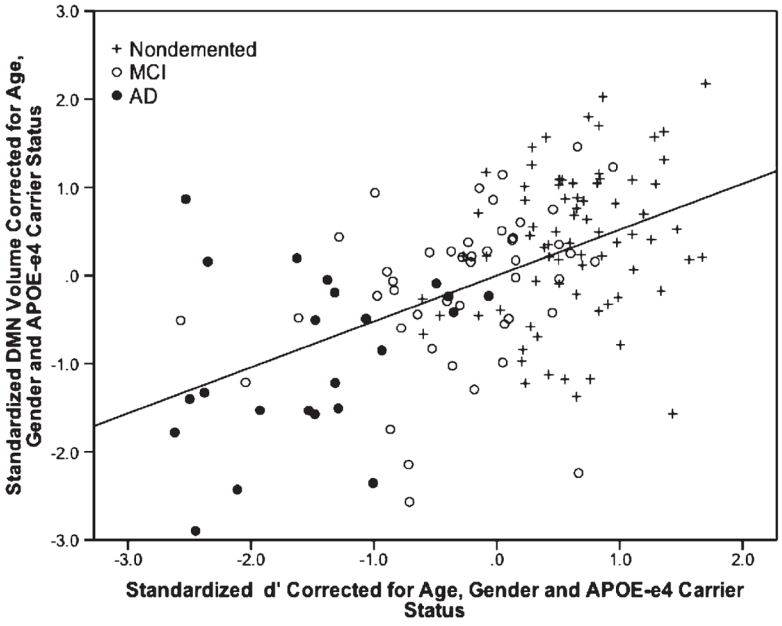

Fig. 4.

Scatterplot of DMN atrophy as a predictor of d scores*. *$r = 0.57$, $p < 0.001$.

$watermark-text
$watermark-text
$watermark-text

$watermark-text
$watermark-text
$watermark-text

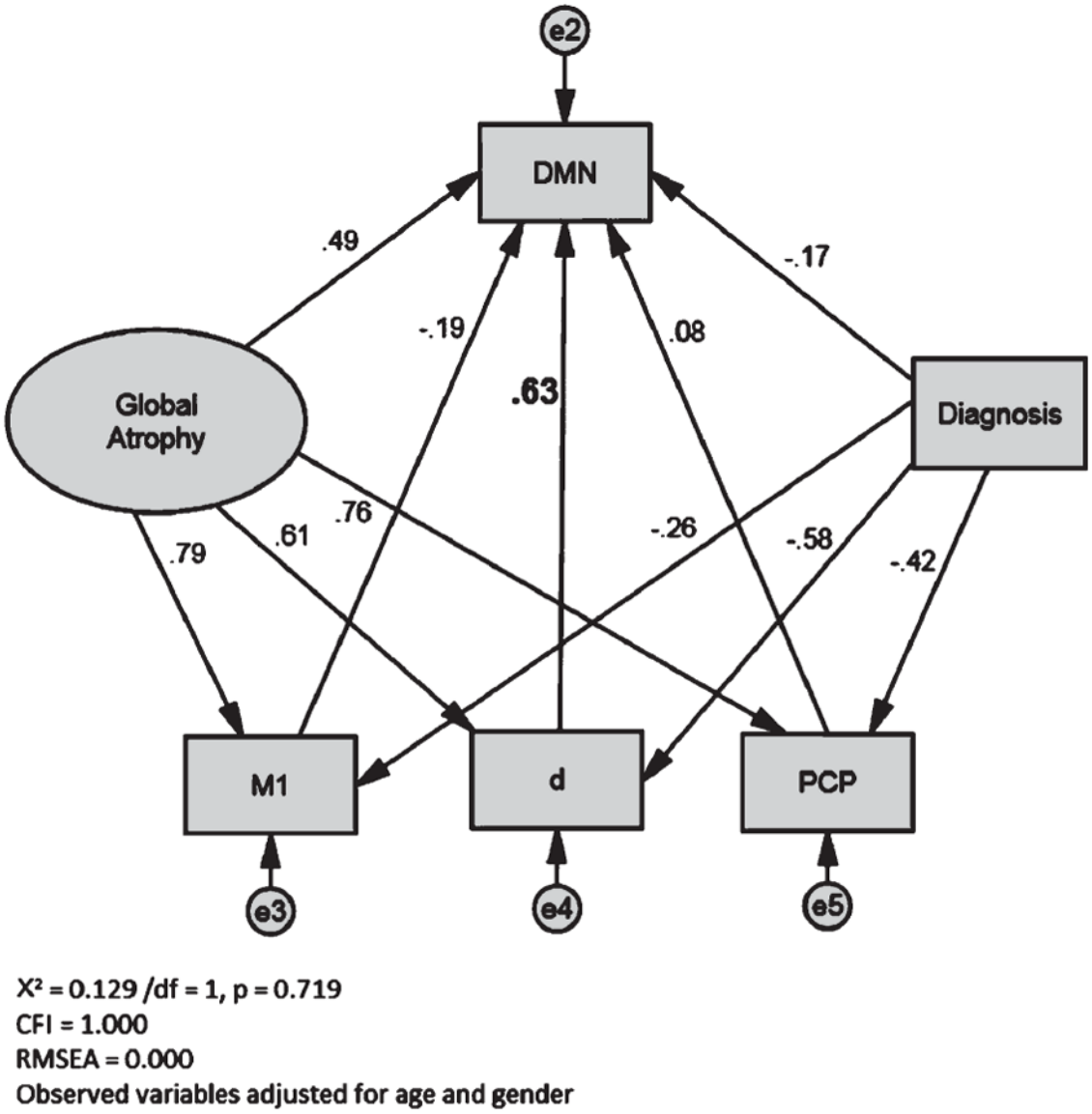

Fig. 5.

The latent variable d is specifically associated with the DMN*. DMN, Default Mode Network eigenvariate, after Bruckner et al., 2009; M1, precentral gyrus eigenvariate; PCP, posterior cingulate/precuneus eigenvariate. *All observed variables are adjusted for age, gender, and APOE $\varepsilon 4$ status. Standardized regression weights are shown. The latent variable d's partial correlaion is significant at $p < 0.001$.

$watermark-text

$watermark-text

$watermark-text

Table 1

Subject characteristics

Variable	Control Mean (SD) (*n* = 76)	MCI Mean (SD) (*n* = 47)	AD Mean (SD) (*n* = 23)	Cognitively impaired Mean (SD) (*n* = 70)
Age (years)	74.2 (7.2)	75.9 (6.5)	73.2 (5.8)	75.0 (6.4)
% Female	58%	62%	70%	64%
% *ε*4 carriers	29.0%	46.8%	73.9%	55.7%
Education (years)	16.3 (2.7)	14.9 (3.2)	15.2 (3.0)	15.0 (3.1)
MMSE	29.4 (0.8)	28.1 (1.3)	22.1 (3.1)	26.1 (3.5)
CDR Global	0	0.5 (0.1)	0.7 (0.3)	0.6 (0.2)
CDR-SB	0 (0.1)	2.7 (1.1)	4.2 (1.2)	3.2 (1.3)

CDR, Clinical Dementia Rating Scale; CDR-SB, CDR Sum of Boxes; MMSE, Mini-Mental State Examination.

$watermark-text

$watermark-text

$watermark-text

Table 2

Raw clinical means

Variable	Control Mean (SD) (*n* = 76)	MCI Mean (SD) (*n* = 47)	AD Mean (SD) (*n* = 23)	Cognitively impaired Mean (SD) (*n* = 70)
LM1	12.9 (4.2)	7.8 (4.5)	3.7 (2.6)	6.5 (4.5)
LMII	10.8 (4.6)	4.6 (4.8)	1.1 (2.0)	3.4 (4.4)
SRTtot	28.3 (6.3)	17.5 (8.8)	6.0 (5.0)	13.7 (9.4)
BNT15	14.2 (1.0)	12.7 (2.7)	9.4 (3.6)	11.6 (3.4)
CFAn	18.6 (4.3)	15.5 (4.5)	9.2 (3.9)	13.4 (5.2)
CFVeg	15.4 (3.7)	11.3 (4.1)	6.3 (2.9)	9.6 (4.4)
BLOCK	33.4 (11.3)	23.9 (10.0)	14.3 (10.3)	20.7 (11.0)
StrCLR	72.0 (11.0)	61.9 (14.8)	44.6 (18.3)	56.2 (17.9)
StrWRD	94.6 (13.6)	81.2 (15.3)	65.0 (20.8)	75.9 (18.8)
StrINT	35.9 (8.7)	27.0 (7.8)	14.5 (8.8)	22.9 (10.0)
Trails A	34.6 (10.5)	54.2 (35.3)	92.9 (49.7)	66.9 (44.2)
Trails B	85.5 (26.0)	139.0 (43.9)	166.9 (22.0)	148.2 (40.2)
ADL	49.4 (2.3)	43.1 (5.4)	36.4 (10.2)	40.9 (7.9)
PPT	30.5 (3.0)	28.5 (2.8)	26.3 (4.3)	27.8 (3.5)

ADL, Alzheimer's Disease Cooperative Study Activities of Daily Living Scale for Mild Cognitive Impairment; BLOCK, WAIS-R Block Design; BNT15, Boston Naming Test (15 item); CFAn, Category Fluency: Animals; CFVeg, Category Fluency: Vegetables; LMI, Wechsler Memory Scale-Revised Logical Memory; LMII, Wechsler Memory Scale-Revised Logical Memory Delayed; PPT, modified Physical Performance Test; SRTtot, Selective Reminding Task Free Recall Total; StrCLR, Stroop Color Task; StrINT, Stroop Color-Word Interference Task; StrWRD, Stroop Task; Trails A, Trail Making Test part A; Trails B, Trail Making Test part B.

$watermark-text

$watermark-text

$watermark-text

Table 3

Model fit

χ^2:df	CMIN	RMSEA	CFI
686.53: 591	1.162	0.033	0.967

$watermark-text

$watermark-text

$watermark-text

Table 4

Latent variable correlations with CDR-SB

Predictor	*r*	*p*
f	0.341	≤0.001
g′	0.171	≤0.001
d	−0.801	≤0.001

$watermark-text $watermark-text $watermark-text

Table 5

Locations of peak correlation of gray matter volume with d*

Region	BA	x	y	z	T	Z	*p* value
Right parahippocampus		29	−36	−8	8.6	7.69	<0.001
Right hippocampus		26	−10	−15	8.1	7.32	<0.001
Right insula	13	40	−3	12	8.77	7.8	<0.001
Right middle cingulate/precuneus	31	5	−54	26	7.61	6.94	<0.001
		7	−49	32	7.38	6.77	<0.001
Right orbital frontal	11	23	30	−17	5.95	5.61	<0.001
		28	37	−13	5.53	5.24	0.002
Left hippocampus/parahippocampus		−26	−39	−8	5.55	5.27	0.002
Left hippocampus		−22	−12	−23	5.75	5.44	0.001
Left insula/middle temporal gyrus	13 & 21	−39	0	7	7.54	6.89	<0.001
		−37	9	5	7.05	6.51	<0.001
		−54	−26	−6	6.31	5.9	<0.001
Left superior middle frontal	11	−6	38	27	7.21	6.63	<0.001
		−7	41	−4	7.09	6.54	<0.001
Left middle cingulate/precuneus	31	−1	−38	34	7.76	7.06	<0.001
Left anterior cingulate	10 & 32	−7	45	15	8.33	7.49	<0.001
Left middle frontal	10	−27	48	26	5.65	5.36	0.001
Left frontal	10	−25	57	5	5.95	5.61	<0.001

*Adjusted for age, gender, APOE-*ε*4 carrier status, g′, and f. Higher d scores are associated with greater gray matter volume in these regions. Family-wise error corrected, minimum cluster size $k = 50$. Bonferonni corrected to $p < 0.003$.